Neuroradiology (2008) 50:171–178
DOI 10.1007/s00234-007-0320-3

INTERVENTIONAL NEURORADIOLOGY

MR angiographic evaluation is limited in intracranial aneurysms embolized with Nexus coils

Hyun-Seung Kang · Won-Jin Moon · Hong Gee Roh · Moon Hee Han · Woo Jin Choe · Joon Cho · Chang-Taek Moon · Young Cho Koh

Received: 23 July 2007 / Accepted: 18 September 2007 / Published online: 25 October 2007

Abstract
Introduction Nexus coils are a type of bioactive coil used to embolize intracranial aneurysms. The purpose of this study was to test the feasibility of the noninvasive follow-up of aneurysms treated with Nexus coils by means of magnetic resonance angiography (MRA).
Methods Three-dimensional (3D) time-of-flight (TOF) MRA images of patients treated with Nexus coils (the Nexus coil group) or bare platinum coils (the control group) were compared for the severity and frequency of artifacts. The reviewers were unaware of the coil types used. In the Nexus coil group, 17 MRA examinations were performed in 14 patients harboring 15 aneurysms treated with Nexus coils using 3-T (n=11) and 1.5-T (n=6) MR units. The findings of these examinations were compared to those of 28 MRA studies conducted on 24 control patients (bare platinum coils). Conventional angiograms, maximum intensity projections, and source data of 3D-TOF MRA were reviewed in terms of residual flow within aneurysms and parent arterial patencies. The qualities of the MRA images were rated from grade 0 (no significant signal loss) to grade 2 (complete segmental signal loss of the parent artery). The normalized ratio, defined as the diameter of signal loss on MRA axial source images (in mm) divided by that of coil mass on plain radiographs (in mm), was calculated to compare the sizes of coil-related artifacts in the two groups.
Results The quality of the MRA image for the Nexus coil group was significantly poorer than that for the control group (p<0.0001) due to signal loss caused by the presence of artifacts in the former. In particular, the interpretation of aneurysmal status was impossible in all cases of coiled aneurysms due to segmental signal loss. The sizes of the MRA artifacts were also significantly larger in the Nexus coil group (normalized ratio 1.61±0.22 vs. 1.15±0.20; p<0.0001).
Conclusion Follow-up evaluations by 3D-TOF MRA of aneurysms treated with Nexus coils are severely limited.

Keywords Coil embolization · Intracranial aneurysm · MR angiography

H.-S. Kang · W. J. Choe · J. Cho · C.-T. Moon · Y. C. Koh
Department of Neurosurgery, Konkuk University Hospital, Seoul, South Korea

W.-J. Moon · H. G. Roh (✉)
Department of Radiology, Konkuk University Hospital, 4-12 Hwayang-dong, Gwangjin-gu, Seoul 143-729, South Korea
e-mail: hgroh@kuh.ac.kr

M. H. Han
Department of Diagnostic Radiology, Seoul National University Hospital, Seoul, South Korea

Introduction

Several types of coils have been developed since the introduction of the Guglielmi detachable coils in 1991 for the treatment of intracranial aneurysms [8, 9] and, more recently, many authors have reported their experiences with bioactive coils for the treatment of intracranial aneurysms [1, 14, 16]. One commercially available type of bioactive coil is the Nexus coil (Micro Therapeutics, Irvine, CA), which is enlaced with an absorbable polymer (polyglycolic acid/lactide copolymer). Our institution has been using Nexus coils to treat intracranial aneurysms since 2006.

Several reports have been published on the noninvasive monitoring of aneurysms treated with coils by magnetic resonance angiography (MRA) and plain radiography [2–6,

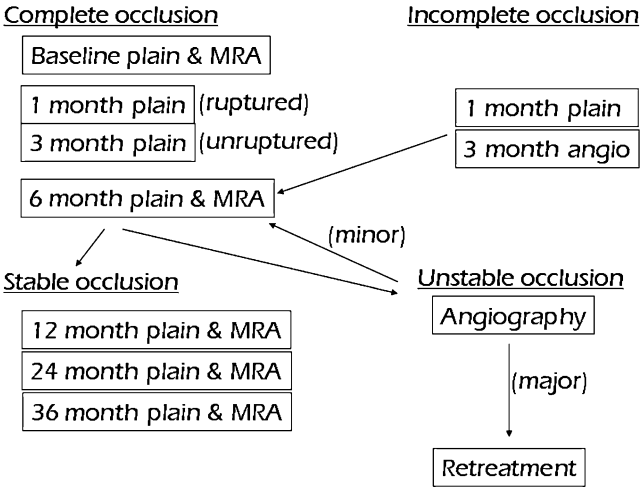

Fig. 1 Follow-up protocol following endovascular coil embolization. *Plain* plain radiography, *MRA* magnetic resonance angiography, *ruptured* ruptured aneurysm, *unruptured* unruptured aneurysm, *major* major recanalization, *minor* minor recanalization

26]. At our institution, patients harboring intracranial aneurysms and treated by coil embolization are evaluated using a predetermined follow-up protocol, which includes plain radiography and MRA at regular intervals as well as conventional angiography, if required (Fig. 1). The purpose of this study was to report three-dimensional (3D) time-of-flight (TOF) MRA findings in a subset of patients treated with Nexus coils, with a focus on the feasibility of noninvasive follow-up. Conventional digital subtraction angiography (DSA) findings were used as a reference standard.

Patients and techniques

Patients

During the period July 2006 to April 2007 we performed endosaccular embolizations using Nexus coils for the treatment of intracranial aneurysms in 19 patients (20 aneurysms). Fourteen of these patients (15 aneurysms: five unruptured and ten ruptured), who underwent 17 MRA examinations after coil embolization, were enrolled in this study (Table 1). The Nexus coils were used in combination with bare platinum coils. The ages of the patients ranged from 39 to 73 years (median 56 years). All of the aneurysms treated, except for one, were less than 10 mm in maximal diameter. There were six internal carotid artery (ICA)–posterior communicating artery aneurysms, four anterior communicating artery aneurysms, three middle cerebral artery aneurysms, one ICA bifurcation aneurysm overriding the A1 segment of the anterior cerebral artery, and one basilar artery bifurcation aneurysm. Three of the 14 patients also underwent coil embolization with bare platinum coils only for additional aneurysms.

Outcomes were assessed using the Glasgow outcome scale (GOS) [12], in which GOS 5 indicates good recovery (resumption of normal life despite minor deficits), GOS 4, moderate disability (disabled but independent), GOS 3, severe disability (conscious but disabled and dependent for daily care), GOS 2, persistent vegetative state (unresponsive and speechless), and GOS 1, death.

Table 1 Characteristics of patients and aneurysms

Patient no./aneurysm no.	Gender/age (years)	H–H grade[a]	Location[b]	Size of aneurysm (mm)	GOS[c]
1/1	F/66	0	MCA	2.9×2.9×1.9	5
2/2	F/48	2	ICA-PCoA	3.8×3.7×2.9	3
3/3	M/60	3	ICA-PCoA	6.6×4.7×3.9	4
4/4[d]	M/39	2	ICA-PCoA	7.1×5.0×4.7	5
5/5	M/52	4	ACoA	3.1×2.9×2.9	5
4/6[d]	M/39	2/0	MCA	4.1×3.8×2.9	5
6/7	M/57	3	ACoA	6.1×3.0×3.9	5
7/8	M/51	2	ACoA	8.7×5.8×5.1	5
8/9	F/71	2	ICA-PCoA	7.8×4.6×4.5	5
9/10	F/53	2	ICA-PCoA	8.4×4.2×3.7	5
10/11	M/68	0	ICA-A1	4.2×3.8×3.6	5
11/12	M/73	0	ACoA	5.2×4.8×4.5	5
12/13	F/55	2	MCA	5.3×4.9×4.0	5
13/14	F/64	0	ICA-PCoA	5.4×4.8×4.1	5
14/15	M/52	3	BA	14.0×6.2×7.2	3

[a] H-H grade, Huns and Hess grade
[b] Location of aneurysm. MCA, Middle cerebral artery; ICA, internal carotid artery, PCoA, posterior communicating artery; ACoA, anterior communicating artery; A1, A1 segment of anterior cerebral artery; BA, basilar artery
[c] GOS, Glasgow outcome scale at the last evaluation
[d] The same patient, in which two aneurysms were treated in separate sessions.

The control group comprised 24 patients with 24 aneurysms (eight unruptured and 16 ruptured). These patients were treated with non-Nexus coils during the same period as the patients treated with the Nexus coils and underwent at least one postembolization MRA. The ages of the patients ranged from 34 to 78 years (median 57 years). All aneurysms, except for one, were less than 10 mm in maximal diameter. There were 11 anterior communicating artery aneurysms, 6 ICA aneurysms, four middle cerebral artery aneurysms, one distal anterior cerebral artery aneurysm, one vertebral artery fenestration aneurysm, and one basilar artery-superior cerebellar artery aneurysm.

Angiography and coil embolization

Digital subtraction angiography and coil embolization were performed using a biplane flat-detector system (Axiom Artis dBA; Siemens Medical System, Erlangen, Germany). Endovascular coil embolization was performed following a standardized protocol in our neuroangiography suite, as described previously [14–18]. General anesthesia was used in all sessions except one. Systemic anticoagulation with heparin was used from the beginning of the procedures in unruptured cases, but only after placing protective packing with coils in cases with a history of recent hemorrhage. Heparin was administered intravenously just after the introducer sheath had been inserted, initially as a 3000-U bolus, then at 1000 U/h. In general, heparin was administered to achieve an activated clotting time of approximately twice the normal rate.

Nexus coils and bare platinum coils were deployed at the operator's discretion (Table 2). Nexus coils were deployed as the last step in eight aneurysms and initially or during the procedure, but not as the final coil, in five aneurysms. Aneurysms were considered to be completely occluded angiographically when the sac and the neck were densely packed, near-completely occluded when the sac was packed but a small neck remained, and incompletely occluded when the sac was persistently opacified [14, 16]. The percentage (%) length of the Nexus coils was calculated following the formula: % length = (total length of Nexus coils deployed into an aneurysm)/(total length of coils deployed into an aneurysm) × 100. In the Nexus coil group, three patients (patients 1, 10, and 13) had other aneurysms that were treated solely with bare platinum coils.

MR angiography

MRA examinations were performed with either a 3-T (Signa HDx; GE Medical Systems, Milwaukee, WI) or a 1.5-T (Signa Excite HD; GE Medical Systems) superconducting MR system; two patients received examinations using both systems. For 3D-TOF MRA, the following parameters were used: for the 1.5-T unit, repetition time (TR), 25 ms; echo time (TE), 6.9 ms; acquisition, 1; flip angle, 20°; matrix, 512×256; effective section thickness,

Table 2 Procedural characteristics of the cases

Aneurysm no.	Coils used in order of deployment[a]	Degree[b]	% Length[c]
1	MH 2–3, NH 2–2	Complete	40
2	Tetris 3–4, MC 2–4	Near complete	50
3	Tetris 5–10, MC 3–7 (2), NH 2–3 (2)	Complete	53
4	MC 4–10, MC 3–7, MC 2–4, NH 2–2	Complete	9
5	Tetris 3–4, GDC10 US 2–1	Near complete	80
6	MC 3–7, MC 2–4, NH 2–1	Near complete	8
7	Morph 3–8, MC 3–7, NH 2–4, MH 2–4	Complete	52
8	Morph 6–12 (2), Morph 5–15, MC 3–7, MC 2–4, MH 2–2	Near complete	75
9	Morph 4–10, Morph 3–8, NH 2–8, MC 2–4 (2)	Near complete	76
10	Morph 3–5 (2), MC 3–7, NH 2–4, MC 2–4, NH 2–2 (2)	Near complete	62
11	Morph 5–18, Morph 3–8, MC 2–4	Near complete	87
12	Morph 5–10, Morph 3–8, MH 3–6, MH 2–4, NH 2–3	Near complete	68
13	Morph 4–10, MC 3–7 (3), MC 2–4 (2), MH 2–3, MH 2–2	Complete	23
14	Tetris 5–10, Morph 3–8, MC 2–4	Incomplete	82
15	TC 12–30, Morph 8–25, TC 7–13, Morph 6–20 (2), TH 6–15, NH 6–20, Morph 5–15 (2), Morph 4–10, Morph 3–8, NH 2–8, NH 2–6	Near complete	72

[a] Coils. MH, Microplex helical coil; MC, Microplex complex coil; NH, Nexus helix supersoft coil; Tetris, Nexus Tetris 3D coil; GDC, Guglielmi detachable coil; US, ultrasoft; Morph, Nexus Morpheus complex coil; TC, Trufill Orbit complex coil; TH, Trufill Orbit helical coil. The dimensions of the coils are expressed as diameter (mm)−length (cm). Numbers in the parentheses denote the number of coils deployed; when a single coil is deployed, the number is omitted.

[b] Degree, Degree of aneurysmal occlusion

[c] % length, % length of Nexus coils among coils deployed into the aneurysm

0.7 mm; field of view (FOV), 240×240 mm; for the 3-T unit, TR, 24 ms; TE, 2.6 ms; acquisition, 1; flip angle, 20°; matrix, 384×224; effective section thickness, 0.6 mm; FOV, 193×220 mm. These parameters are the same as those used during routine MRA for cerebrovascular disease examinations and have been adjusted and optimized to visualize intracranial arterial flow signal.

The anteroposterior (AP) and lateral (that is, left–right) dimensions of signal losses attributed to coiled aneurysms were measured on axial source images showing the largest signal loss using PACS workstation tools (PIVIEWSTAR; Infinitt, Seoul, Korea).

In the Nexus coil group, 3D-TOF MRA examinations were performed between 1 day and 7 months after coil embolization. Intervals between DSA and MRA were 1 week or less in eight examinations, 1 month or less in five, and more than 1 month in four. In the control group, MRA examinations were performed between 1 day and 6 months after coil embolization. Intervals between DSA and MRA were 1 week or less in 16 examinations, 1 month or less in nine, and more than 1 month in three.

Plain radiography

Plain radiography (AP, lateral, and Towne's views) was performed at regular intervals, as shown in Fig. 1. The dimensions of coil masses were measured on the AP and lateral views using PACS workstation tools (PIVIEWSTAR). Lateral dimensions were measured on AP views, and AP dimensions on lateral views.

Image interpretation and analysis

Conventional angiograms, maximum intensity projections (MIP), and source data of 3D-TOF MRA were reviewed separately. Two neuroradiologists (WJM and HGR), both unaware of the coil types employed, determined the residual flow within aneurysms and assessed adjacent vessel patencies by consensus. We rated MRA artifacts as follows: grade 0, no significant signal loss; grade 1, partial signal loss of the parent artery, barely maintaining its continuity; grade 2, complete segmental signal loss of the parent artery. In addition, we calculated the normalized ratio, defined as diameter of signal loss on MRA axial source images (in mm) divided by that of the coil mass on plain radiographs (in mm) in order to estimate and compare the sizes of the coil-related artifacts of Nexus coil cases and controls. As stated previously, AP and lateral dimensions of artifacts and coil masses were used for this calculation. Heights (bottom-to-top dimensions) of MRA artifacts and coil masses were not used because we supposed that heights would have been less accurate as they would have been determined from numbers of involved slices (MRA axial source images). All measurements were performed twice by two neuroradiologists, and average values were used for the statistical analyses.

Results

The percentage lengths of the Nexus coils deployed varied from 8 to 87% (mean ± SD 55.8±25.8) (Table 2). We deployed one Nexus coil each of six aneurysms, two in three aneurysms, three in four aneurysms, five in one aneurysm, and eight in one aneurysm. Coil protrusion into the parent artery was noted in four of 15 aneurysms immediately after embolization. Three-dimensional-TOF MRA examinations were performed using a 3-T MR unit for 11 examinations and the 1.5-T unit for six.

In terms of the MRA artifact grade for the 17 MRA examinations performed in the Nexus coil group, four coiled aneurysms were grade 1 and 13 were grade 2 (Table 3). For the 1.5-T system, one was grade 1 and the other four were grade 2; for the 3-T system, three were grade 1 and eight were grade 2. Consequently, all MRA examinations produced images that were inadequate for accurately evaluating aneurysm status. Illustrative cases are shown in Figs. 2 and 3. In two patients that underwent MRA with both the 3-T and 1.5-T systems, the former provided images with less severe artifacts. Nevertheless, the quality of the images was not good enough to enable interpretation of the aneurysmal status (Fig. 2). No

Table 3 Magnetic resonance angiography artifact grades of the Nexus coil cases

An. No.	Strength of magnetic field (T)	Degree of artifact
1	3 T & 1.5 T	Grade 1 with the 3-T system; Grade 2 with the 1.5-T system
2	1.5 T & 3 T	Grade 2, 1.5-T; Grade 1, 3-T
3	1.5 T	Grade 2
4[a]	1.5 T	Grade 1
5	3 T	Grade 2
6[a]	1.5 T	Grade 2
7	3 T	Grade 1
8	3 T	Grade 2
9	1.5 T	Grade 2
10	3 T	Grade 2
11	3 T	Grade 2
12	3 T	Grade 2
13	3 T	Grade 2
14	3 T	Grade 2
15	3 T	Grade 2

T, Tesla

[a] The same patient, in which two aneurysms were treated in separate sessions.

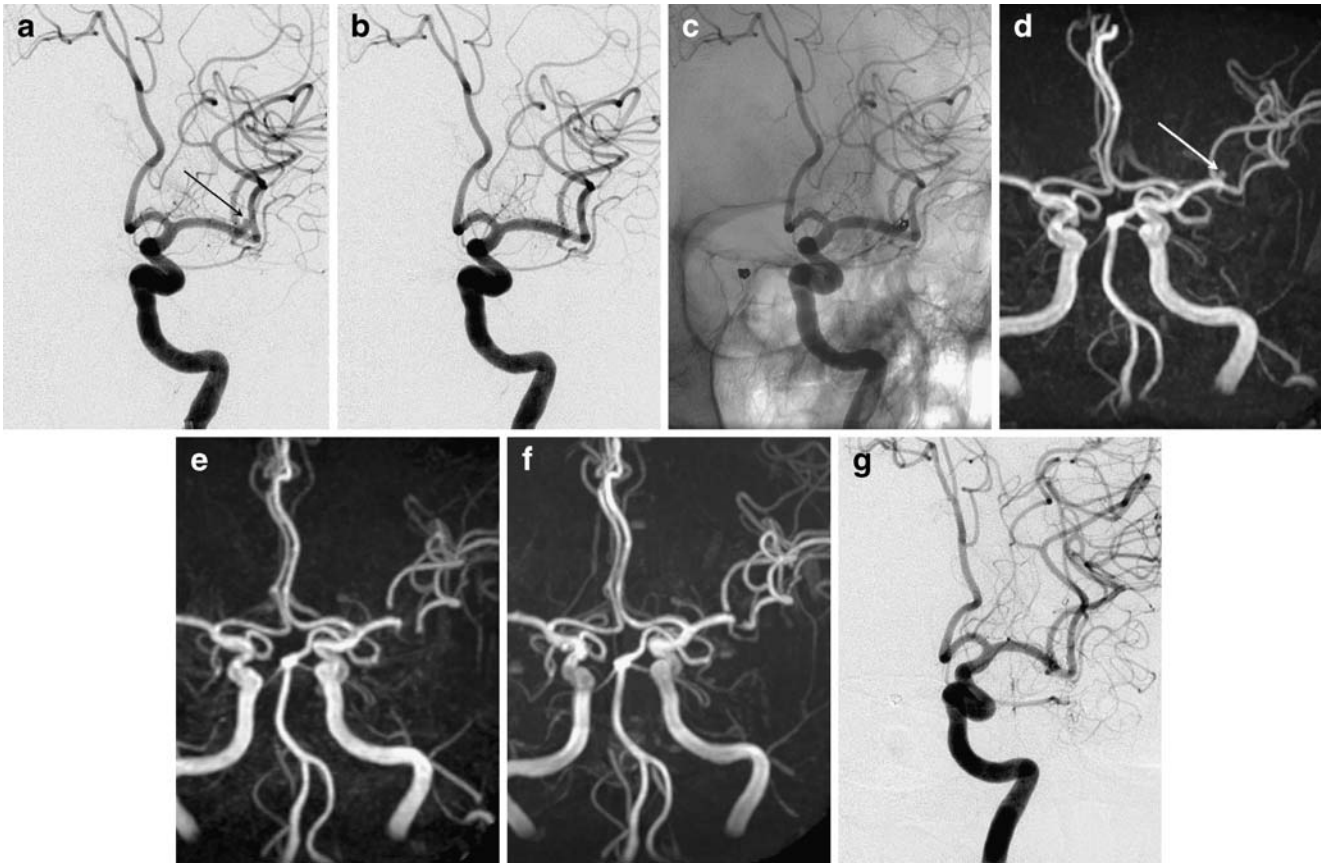

Fig. 2 Images obtained in a 66-year-old woman who underwent coil embolization for an unruptured middle cerebral artery (MCA) aneurysm (No. 1). **a** Pre-embolization angiogram showing a small aneurysm (*arrow*) at the MCA. **b** Post-embolization angiogram. The aneurysm is completely occluded with two coils (Microplex helical 2 mm–3 cm and Nexus Helix supersoft 2 mm–2 cm). **c** Post-embolization unsubtracted angiogram showing a slight protrusion of a loop of the Nexus coil at the aneurysm neck. **d** Pre-embolization three-dimensional (3D) time-of-flight (TOF) image obtained with maximum intensity projection (MIP) reconstruction showing a small aneurysm (*arrow*) at the MCA. **e**, **f** Control 3D-TOF images at 7 and 6 months after the embolization, obtained with a 1.5-T and 3-T MR unit, respectively. Segmental signal losses are observed around the embolized aneurysm, and the signal losses are smaller in the image obtained with a 3-T MR unit (**f**). **g** Control DSA image at 6 months after the embolization showing stable occlusion of the aneurysm without stenosis of the adjacent arteries. A coil loop is found to be protruded at the aneurysm neck

qualitative or quantitative correlation could be found between the volume of the Nexus coils or the locations of aneurysms and degrees of signal losses in the MRA images. A single short Nexus coil was enough to produce significant artifacts in any location.

In the control group (n=28), 24 coiled aneurysms were grade 0, one was grade 1, and three were grade 2. Using the 1.5-T system (n=3), two were grade 0 and one was grade 2; and for the 3-T system (n=25), 22 were grade 0, one was grade 1, and two were grade 2. Thus, a significant difference was observed between the two study groups (p<0.0001) (Table 4).

Three patients in the Nexus coil group had additional aneurysms that were treated with bare platinum coils only. Interpretable MRA images, in terms of aneurysm occlusion, were obtained for aneurysms treated with non-Nexus coils in all of these, while significant signal losses occurred around aneurysms treated with Nexus coils (Fig. 3).

We also measured the MR artifact size in MRA axial source images and the coil mass size in plain radiographs to produce a normalized ratio. The Nexus coil group had significantly larger normalized ratios than the control group at 3 T (p<0.0001) (Table 5).

Discussion

Previous studies have demonstrated that the use of platinum microcoils for intracranial aneurysm embolization is highly compatible with 1.5-T and 3-T MR systems [10, 11, 20, 23]. These coils are nonferromagnetic and do not produce heat, and although they do produce artifacts during MR imaging, these are minimal. Two kinds of MR imaging artifacts were noted in an in vitro evaluation of Guglielmi detachable coils [11] – an elongation of coil mass width in the readout direction on gradient-echo sequences, and a

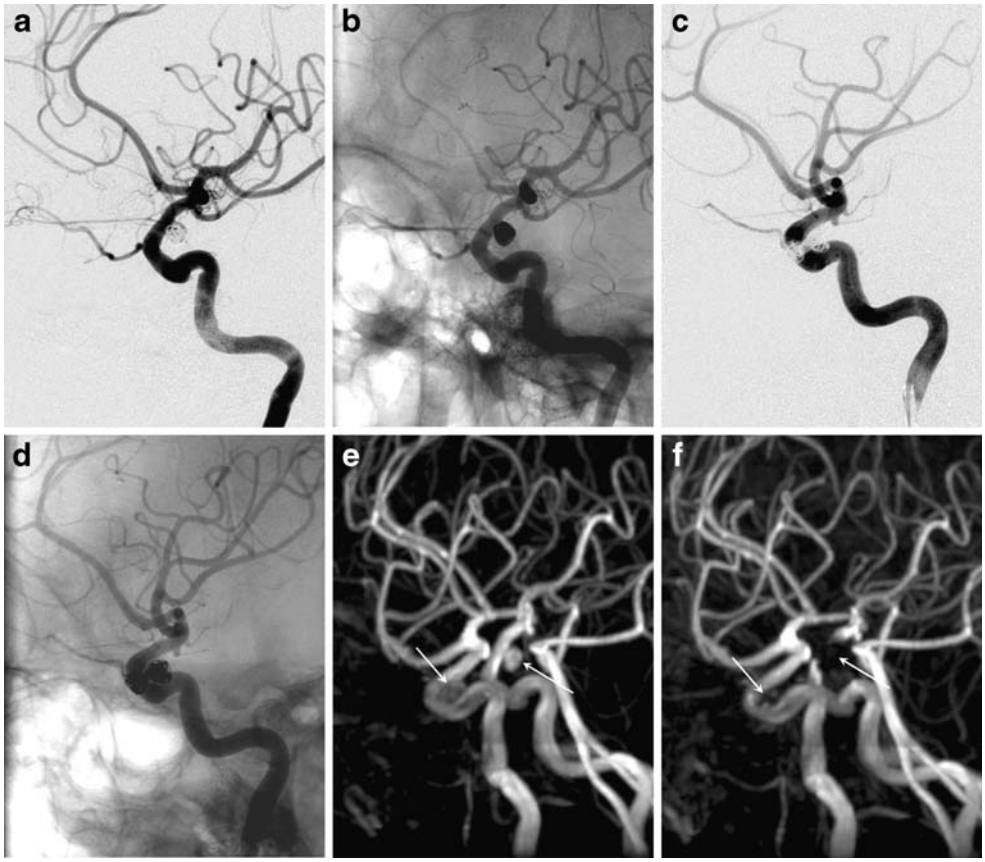

Fig. 3 Images obtained in a 64-year-old woman who underwent coil embolizations for internal carotid artery (ICA) aneurysms (No. 14). **a**, **b** Post-embolization subtracted (**a**) and unsubtracted (**b**) angiograms showing an embolized left ICA aneurysm at the posterior communicating artery level. The aneurysm is incompletely occluded with three coils (Nexus Tetris 3D 5 mm–10 cm, Nexus Morpheus complex 3 mm–8 cm, Micoplex complex 2 mm–4 cm). **c**, **d** Post-embolization subtracted (**c**) and unsubtracted (**d**) angiograms showing an embolized right paraclinoid ICA aneurysm. The aneurysm is completely occluded with four coils (Microplex complex 5 mm–12 cm, Microplex helical 4 mm–8 cm, Microplex complex 2 mm–4 cm, Microplex helical 2 mm–4 cm) at the same session. **e**, **f** Pre- and post-embolization 3D-TOF images obtained with a 3-T MR unit. A segmental signal defect is shown at the left ICA while the right ICA is well-visualized with stable occlusion of the aneurysm (*arrows*)

hyperintense rim adjacent to coil mass, which was most apparent on fast spin-echo images and at higher echo time values. In human subjects, a rim of increased intensity adjacent to a 2- to 3-mm area of signal void and obscuration surrounding brain parenchyma has been observed [10].

To our knowledge this is the first report of MRA findings related to Nexus coils. Our study shows that segmental signal losses of parent arteries and coiled aneurysms made evaluations of aneurysms impossible by 3D-TOF MRA. In the present series, the presence of segmental signal loss did not depend on the percentage lengths of the Nexus coils in the aneurysms or on the presence of coil protrusion into the parent artery. In six cases, only one Nexus coil was enough to significantly disrupt the MRA images. The 3-T MR unit seemed to produce better images with lower signal losses than the 1.5-T unit, although even these images were not useful, as

Table 4 Comparison of Nexus coil group and control group according to MRA artifact grades[a]

Group	Grade 0 (*n*)	Grade 1 (*n*)	Grade 2 (*n*)	Total (*n*)
Nexus	0	4	13	17
Control	24	1	3	28

[a] Fisher's exact test, $p<0.0001$ (Odds ratio, 190.56; 95% confidence interval 9.619, 3774.9) for Grade 0 vs. Grades 1 and 2

Table 5 Comparison of the normalized ratio (NR) between the Nexus coil group and control group at 3 T[a]

	Nexus (*n*=11)	Control (*n*=24)	*p*[b]
NR in the lateral dimension	1.62±0.26	1.15±0.22	<0.0001
NR in the anteroposterior dimension	1.59±0.17	1.14±0.18	<0.0001
NR, total	1.61±0.22	1.15±0.20	<0.0001

[a] The normalized ratio is defined as dimension of signal loss on the MRA axial source images (in mm) divided by the dimension of coil mass on plain radiographs (in mm).
[b] unpaired *t* test

they provided no information on the degree of aneurysm occlusion or recanalization.

By comparing normalized ratios, we also found that the sizes of the coil artifacts were significantly larger in aneurysms treated with Nexus coils than in the controls. The causes of these larger artifacts are not obvious. As nonferromagnetic devices become paramagnetic, possible explanations for this phenomenon include the metallurgical compositions of alloys, the degree of cold working, and heat treatment during manufacture [11]. We believe that the artifacts of Nexus coils are due to the metal alloys used – the coils are composed of a platinum–iridium alloy, whereas a platinum–tungsten alloy is usually used for other detachable coils for intracranial aneurysm embolization. In addition, Nexus coils have a Nitinol core.

The MR characteristics of the platinum–iridium alloy have been previously reported [13, 21]. In one of these studies, the apparent size of a platinum–iridium electrode in the MR images increased from 0.5 to 2.2 mm in diameter [13]. The authors concluded that the paramagnetic nature of the platinum–iridium alloy disrupted B_0 homogeneity and that this caused the artifact signals. In another study, the MR images of the platinum–iridium microwires, acquired at 2 T, showed complete signal loss over a region that was substantially larger than the volume occupied by the microelectrodes [21]. For example, a 25-μm platinum–iridium microwire was transformed to a void with a diameter of approximately 500 μm.

Nitinol, however, does not appear to cause significant artifacts in MR images. In an evaluation of stented intracranial arteries, MRA after the placement of Nitinol stents depicted the intracranial artery lumen without distortion or signal loss, whereas stainless-steel stents caused segmental signal loss [19]. Therefore, the platinum–iridium alloy, rather than the Nitinol core, appears to be the major cause of the MR artifacts observed in the present series.

In two Nexus coil cases, 3-T MRA images showed smaller susceptibility artifacts and a better quality of the image than the 1.5-T images (Fig. 2, Table 3). For metallic materials, whether MR compatible or not, the extent of the susceptibility and the radiofrequency of the artifacts are expected to be higher at 3 T than at 1.5 T [25]. We performed MRA at 1.5 T and 3 T using almost the same parameters, except for TE (6.9 ms vs. 2.6 ms). A decrease in the TE is expected to increase signal intensity due to less dephasing and, thereby, reduce magnetic susceptibility artifacts [7, 22]. According to an experimental study, 3-T MRA images had larger artifacts than 1.5-T images when the same TE was applied [24]. Therefore, better image quality with fewer artifacts at 3 T in our study might have been due to a shorter TE and to an increased signal-to-noise ratio at 3 T. Thus, 1.5-T MRA with a short TE may provide images with less severe artifacts than 3-T MRA.

MR angiography has a central role during the noninvasive follow-up of coiled aneurysms [3–6, 26]. However, at the present time it does not appear to be suitable in cases treated with Nexus coils, which can limit the use of these coils in clinical practice. Further research aimed at improving MRA quality in cases treated with Nexus coils is required.

Conclusion

Magnetic resonance angiography images of intracranial aneurysms treated with Nexus coils showed significantly more severe artifacts than those of intracranial aneurysms treated with bare platinum coils. These artifacts hinder the noninvasive follow-up of coiled aneurysms.

Conflict of interest statement We declare that we have no conflict of interest.

References

1. Bendszus M, Solymosi L (2006) Cerecyte coils in the treatment of intracranial aneurysms: a preliminary clinical study. AJNR Am J Neuroradiol 27:2053–2057
2. Connor SE, West RJ, Yates DA (2001) The ability of plain radiography to predict intracranial aneurysm occlusion instability during follow-up of endosaccular treatment with Guglielmi detachable coils. Neuroradiology 43:680–686
3. Costalat V, Lebars E, Sarry L, Defasque A, Barbotte E, Brunel H, Bourbotte G, Bonafe A (2006) In vitro evaluation of 2D-digital subtraction angiography versus 3D-time-of-flight in assessment of intracranial cerebral aneurysm filling after endovascular therapy. AJNR Am J Neuroradiol 27:177–184
4. Cottier JP, Bleuzen-Couthon A, Gallas S, Vinikoff-Sonier CB, Bertrand P, Domengie F, Barantin L, Herbreteau D (2003) Intracranial aneurysms treated with Guglielmi detachable coils: is contrast material necessary in the follow-up with 3D time-of-flight MR angiography? AJNR Am J Neuroradiol 24:1797–1803
5. Cottier JP, Bleuzen-Couthon A, Gallas S, Vinikoff-Sonier CB, Bertrand P, Domengie F, Barantin L, Herbreteau D (2003) Follow-up of intracranial aneurysms treated with detachable coils: comparison of plain radiographs, 3D time-of-flight MRA and digital subtraction angiography. Neuroradiology 45:818–824
6. Derdeyn CP, Graves VB, Turski PA, Masaryk AM, Strother CM (1997) MR angiography of saccular aneurysms after treatment with Guglielmi detachable coils: preliminary experience. AJNR Am J Neuroradiol 18:279–286
7. Gonner F, Heid O, Remonda L, Nicoli G, Baumgartner RW, Godoy N, Schroth G (1998) MR angiography with ultrashort echo time in cerebral aneurysms treated with Guglielmi detachable coils. AJNR Am J Neuroradiol 19:1324–1328
8. Guglielmi G, Vinuela F, Dion J, Duckwiler G (1991) Electrothrombosis of saccular aneurysms via endovascular approach. Part 2: Preliminary clinical experience. J Neurosurg 75:8–14
9. Guglielmi G, Vinuela F, Sepetka I, Macellari V (1991) Electrothrombosis of saccular aneurysms via endovascular approach. Part 1: Electrochemical basis, technique, and experimental results. J Neurosurg 75:1–7
10. Hartman J, Nguyen T, Larsen D, Teitelbaum GP (1997) MR artifacts, heat production, and ferromagnetism of Guglielmi detachable coils. AJNR Am J Neuroradiol 18:497–501
11. Hennemeyer CT, Wicklow K, Feinberg DA, Derdeyn CP (2001) In vitro evaluation of platinum Guglielmi detachable coils at 3 T

with a porcine model: safety issues and artifacts. Radiology 219:732–737
12. Jennett B, Bond M (1975) Assessment of outcome after severe brain damage: a practical scale. Lancet 1:480–484
13. Jupp B, Williams JP, Tesiram YA, Vosmansky M, O'Brien TJ (2006) MRI compatible electrodes for the induction of amygdala kindling in rats. J Neurosci Methods 155:72–76
14. Kang HS, Han MH, Kwon BJ, Kwon OK, Kim SH, Choi SH, Chang KH (2005) Short-term outcome of intracranial aneurysms treated with polyglycolic acid/lactide copolymer-coated coils compared to historical controls treated with bare platinum coils: a single-center experience. AJNR Am J Neuroradiol 26:1921–1928
15. Kang HS, Han MH, Kwon BJ, Kwon OK, Kim SH (2006) Repeat endovascular treatment in post-embolization recurrent intracranial aneurysms. Neurosurgery 58:60–70
16. Kang HS, Han MH, Lee TH, Shin YS, Roh HG, Kwon OK, Kwon BJ, Kim SY, Kim SH, Byun HS (2007) Embolization of intracranial aneurysms with hydrogel-coated coils: result of Korean Multicenter Trial. Neurosurgery 61:51–59
17. Kwon BJ, Han MH, Oh CW, Kim KH, Chang KH (2002) Anatomical and clinical outcomes after endovascular treatment for unruptured cerebral aneurysms: a single center experience. Interv Neuroradiol 8:367–376
18. Kwon BJ, Han MH, Oh CW, Kim KH, Chang KH (2003) Procedure-related haemorrhage in embolisation of intracranial aneurysms with Guglielmi detachable coils. Neuroradiology 45:562–569
19. Lovblad KO, Yilmaz H, Chouiter A, San Millan Ruiz D, Abdo G, Bijlenga P, de Tribolet N, Ruefenacht DA (2006) Intracranial aneurysm stenting: follow-up with MR angiography. J Magn Reson Imaging 24:418–422
20. Marshall MW, Teitelbaum GP, Kim HS, Deveikis J (1991) Ferromagnetism and magnetic resonance artifacts of platinum embolization microcoils. Cardiovasc Intervent Radiol 14:163–166
21. Martinez-Santiesteban FM, Swanson SD, Noll DC, Anderson DJ (2007) Magnetic field perturbation of neural recording and stimulating microelectrodes. Phys Med Biol 52:2073–2088
22. Schmalbrock P, Yuan C, Chakeres DW, Kohli J, Pelc NJ (1990) Volume MR angiography: methods to achieve very short echo times. Radiology 175:861–865
23. Shellock FG, Detrick MS, Brant-Zawadski MN (1997) MR compatibility of Guglielmi detachable coils. Radiology 203:568–570
24. Walker MT, Tsai J, Parish T, Tzung B, Shaibani A, Krupinski E, Russell EJ (2005) MR angiographic evaluation of platinum coil packs at 1.5 T and 3 T: an in vitro assessment of artifact production: technical note. AJNR Am J Neuroradiol 26:848–853
25. Wall A, Kugel H, Bachman R, Matuszewski L, Kramer S, Heindel W, Maintz D (2005) 3.0 T vs. 1.5 T MR angiography: in vitro comparison of intravascular stent artifacts. J Magn Reson Imaging 22:772–779
26. Yamada N, Hayashi K, Murao K, Higashi M, Iihara K (2004) Time-of-flight MR angiography targeted to coiled intracranial aneurysms is more sensitive to residual flow than is digital subtraction angiography. AJNR Am J Neuroradiol 25:1154–1157